ELSEVIER

Solid State Ionics 149 (2002) 11–19

SOLID STATE IONICS

www.elsevier.com/locate/ssi

$Sm_{0.5}Sr_{0.5}CoO_3$ cathodes for low-temperature SOFCs

Changrong Xia, William Rauch, Fanglin Chen, Meilin Liu *

School of Materials Science and Engineering, Georgia Institute of Technology, Atlanta, GA 30332-0245, USA

Received 17 September 2001; received in revised form 1 February 2002; accepted 11 February 2002

Abstract

The electrochemical properties of the interfaces between an $Sm_{0.2}Ce_{0.8}O_{1.9}$ (samaria-doped ceria, SDC) electrolyte and porous composite cathodes consisting of $Sm_{0.5}Sr_{0.5}CoO_3$ (SSC) and SDC have been investigated in anode-supported single cells at low temperatures (400–600 °C). The bilayer structures of the SDC electrolyte films (25 μm thick) and the NiO–SDC anode supports were formed by co-pressing and subsequent co-firing at 1350 °C for 5 h. The effect of composition, firing temperature, and microstructure of the composite cathodes on the electrochemical properties is systematically studied. Results indicate that the optimum firing temperature is about 950 °C, whereas the optimum content of SDC electrolyte in the composite cathodes is about 30 wt.%. It is noted that the addition of the proper amount of SDC to SSC dramatically improved the catalytic properties of the interfaces; reducing the interfacial resistance by more than one order of magnitude compared with an SSC cathode without SDC.

Keywords: Solid oxide fuel cells; Low-temperature SOFC; Strontium-doped samarium cobaltite; Interfacial resistance; Cathode

1. Introduction

It is desirable to lower the operating temperature of solid oxide fuel cells (SOFCs) from around 1000 to below 600 °C. The lower operating temperature would solve various problems associated with the high temperature operation, such as densification of electrodes, formation of an insulating layer at the electrode/electrolyte interface by interdiffusion, and crack formation from stress caused by large differences in the thermal expansion coefficients of the cell components. Besides, low operating temperature will extend the range of material selection for cell components such as the interconnect and cell housing. The reduction of operation temperature can be achieved either by thinning the electrolyte layer, or by using highly conductive electrolytes, such as doped cerias [1–5]. When a cell is operated at temperatures below 550 °C using doped ceria electrolytes (thinner than 30 μm), the cathode becomes critical for the fuel cell performance since the activation energy for cathodic reaction is very large. The ratio of the cathodic resistance to electrolyte resistance varied from 0.7 at 550 °C to 8.5 at 400 °C for a cell based on a 30-μm-thick $Sm_{0.2}Ce_{0.8}O_{1.9}$ (samaria-doped ceria, SDC) electrolyte [4].

$La_{1-x}Sr_xMnO_3$ perovskite (LSM) is regarded as one of the most promising cathode materials for SOFCs because of its high thermal and chemical stability [6]. While LSM has shown promising performance for SOFCs operating at temperatures above

* Corresponding author. Tel.: +1-404-894-6114; fax: +1-404-894-9140.

E-mail address: meilin.liu@mse.gatech.edu (M. Liu).

0167-2738/02/$ - see front matter
PII: S0167-2738(02)00131-5

800 °C, its performance decreases rapidly as the operating temperature decreases. Considerable improvements in LSM-based cathodes have, therefore, been engineered into SOFCs designed to operating within the range of 600–800 °C by the use of dual phase cathodes or by improvements in the cathode microstructure. For instance, with 50 wt.% Gd-doped ceria (GDC), LSM yielded 0.34 Ω cm^2 interfacial resistance at 750 °C in air using GDC as electrolyte [7]. At 600 °C, it increased to 4.44 Ω cm^2, which is about 36 times higher than the resistance of a 30-μm-thick GDC [7,8]. It seems very likely that only limited improvements of LSM cathodes will be realized because the oxygen surface exchange coefficient and oxygen diffusion coefficient values of LSM are relatively low [8,9]. Considerable research interest is, therefore, currently directed towards cobalt-containing perovskite oxides, which tend to exhibit higher ionic conductivities than LSM due to a greater concentration of oxygen vacancies [8,10,11]. Interest has especially grown in the Sr-doped $LaCoO_3$ (LSC) compositions, where interfacial resistances of ~ 0.6 and < 0.1 Ω cm^2 were observed at 590 and 690 °C, respectively, for a $La_{0.4}Sr_{0.6}Co_{0.2}Fe_{0.8}O_3$ (LSCF) cathode containing 30 wt.% GDC on GDC electrolyte [11]. It is believed that an interfacial resistance as low as 0.2 Ω cm^2 at around 600 °C can be achieved with LSCF/GDC composite cathodes by further improving the microstructure and composition [8].

Strontium-doped samarium cobaltite with composition of $Sm_{0.5}Sr_{0.5}CoO_3$ (SSC) has been studied as a cathode material for SOFCs with yttria stabilized zirconia (YSZ), $La_{1-x}Sr_xGa_{1-y}Mg_yO_3$, and doped ceria electrolytes [3–5,12–14]. Dense SSC showed ~ 50% lower overpotential than LSC under similar conditions. The rate-determining step of dense SSC cathodes was shown to be adsorption–desorption at the surface of the electrode, the same as LSC. But the adsorption and desorption rate constants of SSC were approximately one order of magnitude larger than the corresponding values of LSC. Furthermore, the electrochemical performance of SSC porous cathodes can be improved by adding doped ceria, which results in the suppression of growth of SSC particles, thereby maintaining the porosity and increasing the triple phase boundaries. The performance can also be improved by optimizing the connectivity and size distribution between particles of each solid phase to yield a larger three-phase (cathode–electrolyte–gas) contract area that is accessible for oxygen reduction. Besides, SSC is compatible both chemically and physically with ceria electrolyte. In this work, SSC was synthesized using a glycine–nitrate process. Interfacial resistance of the SSC cathode and samaria-doped ceria (SDC), as well as cathodic overpotential were investigated in regards to the firing temperature and the amount of SDC in the composite cathodes.

2. Experimental procedures

$Sm_{0.5}Sr_{0.5}CoO_3$ (SSC) powders were prepared by the glycine–nitrate method [15]. Stoichiometric amount of $Sm(NO_3)_3{\cdot}6H_2O$ (99.9%), $Sr(NO_3)_2$ (99.0%), and $Co(NO_3)_2{\cdot}6H_2O$ (98.5%) were dissolved in distilled water to form an aqueous solution, to which glycine (0.5 mol glycine per mol NO_3^-) was then added in solid state. Combustion of the metal nitrate/glycine solution was subsequently performed in glass beakers on a hotplate, with approximately 20 ml of the precursor solution (0.02 mol with respect to cobalt) burned at a time. The precursors were heated to evaporate excess water, yielding a red viscous liquid. Further heating caused the viscous liquid to autoignite, resulting in rapidly and self-sustaining combustion. The resultant black ash was then collected and heated in air at 800 °C for 2 h to remove the carbon residue and to convert it to the desired $Sm_{0.5}Sr_{0.5}CoO_3$ phase of perovskite structure, as measured by X-ray diffraction (PW-1800).

The electrochemical performance of the SSC powder as a cathode for a low-temperature SOFC was characterized in a samaria-doped ceria ($Sm_{0.2}Ce_{0.8}O_{1.9}$, SDC)-based fuel cell. The cell was fabricated by a dry-pressing process utilizing a highly porous SDC powder, prepared by the glycine–nitrate method and calcined at 600 °C for 2 h [3]. To make a single cell, a mixed powder of SDC and NiO (65 wt.%) was pressed at 200 MPa as a substrate (~ 25 mm in diameter and 0.5 mm thick), SDC powder was then added, distributed uniformly, and pressed onto the substrate at 250 MPa. The bilayer was subsequently sintered at 1350 °C for 5 h, resulting in an SDC film of about 25 μm thick on an SDC/NiO substrate; upon exposure to a reducing atmosphere (such as a hydro-

gen fuel), the NiO is reduced to metallic Ni, resulting in a porous SDC/Ni anode, with porosity, Ni and SDC volume fractions of over 30%.

SSC was mixed with 10 wt.% SDC and applied to the electrolyte film as a cathode by painting (a Heraeus organic binder V006). The painted slurries were then dried and fired at 900, 950, and 1000 °C in air for 4 h with heating and cooling rates of 300 °C/h to investigate the effect of the sintering temperature on the SSC cathode performance. Different amounts of SDC (0–40 wt.%) were mixed with SSC and applied to the electrolyte to investigate the effect of SDC content on the electrochemical performance of the cathode. The cathodes were named, for example, as SSC–SDC10(950), which means the cathode was consisted of SSC and 10 wt.% SDC, and fired at 950 °C for 4 h. The cathode area was about 0.8 cm^2 and the thickness was about 40 μm for a cathode fired at 950 °C.

A silver reference electrode was prepared by painting silver paste (Heraeus 8710) onto the electrolyte (cathode side, about 2 mm away from the edge) and firing at 700 °C for 1 h. A silver current collector was made onto the cathode surface by painting a square pattern in the center of the cathode using the silver paste. In general, accurate determination of electrode polarization resistances using a three-electrode configuration requires careful cell design. While the best cell configuration appears to be the one with the counter and the working electrode being of the same size and shape to ensure a uniform current distribution, it is difficult to achieve in reality [16]. A better configuration, in practice, is the one used in this experiment, an anode-supported single cell in which the anode (the counter electrode) is much bigger than the cathode (the working electrode) and the cathode is in the center of the cell (or against the center of the anode). In this case, the entire cathode area is active and the current distribution is symmetrical about the center. As a result, the cathode–electrolyte interface as well as the exact active area of the cathode is well defined. It is noted, however, that this configuration would not be appropriate for investigation of the anode–electrolyte interface.

Electrochemical characterizations were performed from 400 to 600 °C under ambient pressure. Humidified (3 vol.% H_2O) hydrogen was used as fuel and stationary air as oxidant. Fuel cell performances were measured with an EG&G Potentiostat/Galvanostat (Model 273A) with a computer interface. Current–voltage (I–V) characteristics of the cells were measured using Linear Sweep Voltammetry at a sweep rate of typically 1 mV/s. The impedances were typically measured in the frequency range from 0.1 Hz to 100 kHz using an EG&G lock-in amplifier (model 5210) in combination with the EG&G Potentiostat/Galvanostat and the computer interface. The cathode (SSC–SDC) was used as working electrode, anode (Ni–SDC) as counter, with the silver as reference electrode. Overpotentials were calculated using data from the Linear Sweep Voltammetry and the impedance spectra measurements.

In order to investigate the phase structures and specific area of the cathodes, the slurries consisting of SSC and SDC were also painted onto alumina substrates and fired under the same conditions as for the cathodes. The fired structure and phase purity of the SSC–SDC composites, removed from the alumina substrates, were studied using X-ray diffraction (XRD, PW-1800 system, with Cu-Kα radiation operated at 40 kV and 30 mA, and a 2θ scanning rate of 0.2°/min). Specific surface area of the SSC powder was measured by an isothermal nitrogen adsorption–desorption measurement (Coulter SA3100). The morphologies of the tested cathodes were revealed using a scanning electron microscope (SEM, Hitachi S-800).

3. Results and discussion

3.1. Structure and microstructure of SSC

Observation under SEM revealed that the ash consisted of highly porous particles, most of which were linked together in chains. The specific area of the ash was 27.1 m^2/g as determined by the BET measurement. Heating the ash to 800 °C for 2 h decreased the specific area to 3.43 m^2/g. The as-prepared ash was amorphous as determined by the XRD measurement. Calcinating above 800 °C converted the amorphous ash to the perovskite structure as shown in Fig. 1. The same structure was observed on SSC prepared by solid-state reaction. No obvious chemical or solid-state reactions between SSC and SDC were revealed from the XRD patterns for the composites heated up to 1000 °C in air for 4 h, regardless of the content of

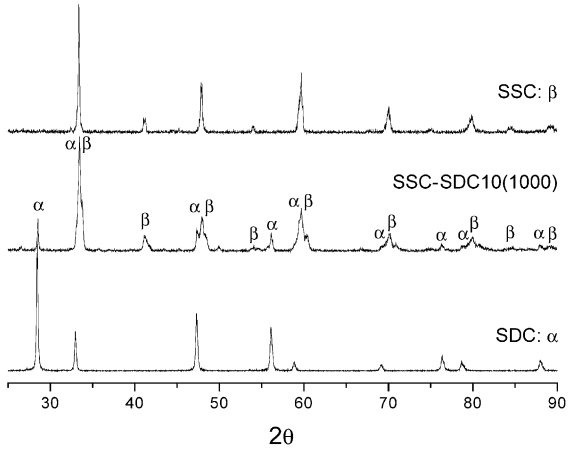

Fig. 1. X-ray diffraction patterns of $Sm_{0.2}Ce_{0.8}O_{1.9}$ (SDC, fired at 1000 °C 2 h), $Sm_{0.5}Sr_{0.5}CoO_3$ (SSC, fired at 1000 °C 2 h), and composite (SSC–SDC10(1000)) consisted of SSC + 10 wt.% SDC (fired at 1000 °C for 4 h).

SDC in the composites. For example, Fig. 1 shows that only SDC and SSC patterns could be identified on the XRD pattern of SSC–SDC10(1000). However, phases other than perovskite SSC and fluorite SDC were present when the composite was fired at 1250 °C for 4 h. While the long-term stability of SSC–SDC composites needs to be further studied, it seems that SSC is a chemically stable cathode material for fuel cells based on doped ceria when the firing temperature is below 1000 °C and the anticipated operating temperature is below 700 °C.

3.2. Open circuit voltages (OCVs)

Shown in Fig. 2 are the temperature dependences of OCV (V_{OC}) for a hydrogen/air fuel cell based on a 0.4-mm-thick SDC, and the ratio of OCV to Nernst potential (E_N), V_{OC}/E_N. OCV decreased rapidly from 1.08 V at 400 °C to about 0.90 V at 650 °C due to increased electronic conduction in the SDC electrolyte at high temperatures under fuel cell conditions. It is also noted that the OCVs across the cell with a thinner electrolyte (30 μm thick) were lower than those across the cell with a thicker electrolyte (0.4 mm thick). This is because OCVs depend also on the thickness of an electrolyte with partial electronic conductivity (such as SDC under the fuel cell conditions); the thinner the electrolyte, the lower the OCV [17]. Since the electronic conduction in SDC is not negligible under the fuel cell conditions, the interfacial resistances R_p of the fuel cells based on SDC are determined with the following equation [18],

$$R_p = \frac{R_T - R_b}{\frac{V_{OC}}{E_N}\left[1 - \frac{R_b}{R_T}\left(1 - \frac{V_{OC}}{E_N}\right)\right]}$$

where R_T is the total resistance of the fuel cell as determined from the intercept of the impedance loop with the real axis at low frequencies, R_b is the resistance of the bulk electrolyte obtained from the intercept at high frequencies, V_{OC} is the open cell voltage, and E_N is the Nernst potential across the cell.

3.3. Effect of firing temperature on interfacial properties

Shown in Fig. 3 are the impedance spectra obtained at 600 °C for a cathode consisting of SSC + 10 wt.% SDC, fired at 950 °C for 4 h, under the influence of an applied DC voltage of 0, − 100, − 200, and − 300 mV versus open circuit voltage. The intercepts of the impedance arcs with the real axis at high frequencies correspond to the resistance of the electrolyte and the lead wires. Clearly, the interfacial impedance decreased with the amplitude of the applied DC voltage. For the A-site-doped perovskite oxygen ion and electronic-mixed conducting materials, the oxygen ion transfer resistance is dependent on oxygen vacancy concentration, $[V_o^{\cdot\cdot}]$, which depends

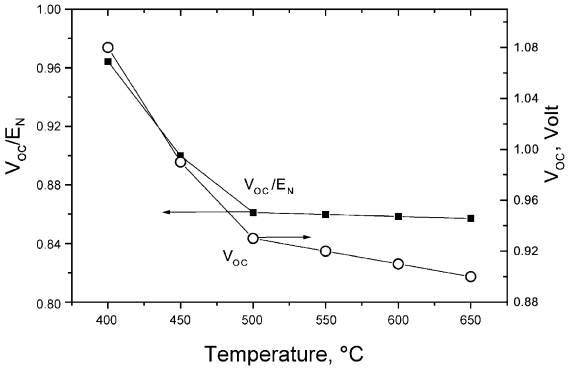

Fig. 2. Open cell voltages (OCVs) for a fuel cell based on SDC (0.4 mm thick) with humidified hydrogen (3 vol.% H_2O) as fuel and air as oxidant and the ration of OCVs to the Nernst potential (E_N).

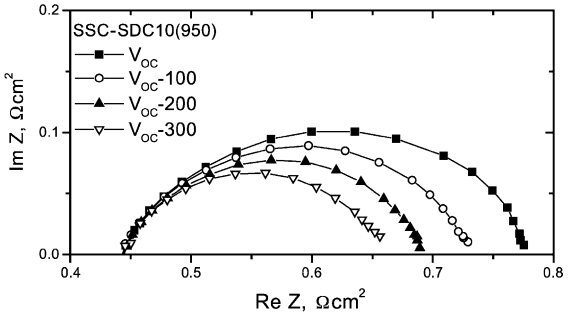

Fig. 3. Impedance spectra for the SSC–SDC10(950) cathode at 600 °C at DC voltages of open cell voltage (V_{OC}), V_{OC} − 100, V_{OC} − 200, and V_{OC} − 300 mV.

critically on the local oxygen partial pressure, P_{O_2}, according to [10]

$$[V_o^{\cdot\cdot}] \propto P_{O_2}^{-1/4}.$$

High P_{O_2}, which is equivalent to a low cathodic overpotential, corresponds to low oxygen vacancy concentration, and thus low oxygen conductivity or high resistance. Conversely, low P_{O_2} is equivalent to a high cathodic overpotential, and thus low cathodic resistance is expected.

Fig. 4 shows the overpotential at 500 and 600 °C for SSC–SDC10 cathodes fired at 900, 950, and 1000 °C for 4 h. The interfacial impedance spectra of the cathodes at open circuit voltage as measured using a three-electrode configuration are shown in Fig. 5. It is very clear from Figs. 4a and 5 that at 600 °C, SSC–SDC10 fired at 950 °C had the best electrochemical performances: the lowest overpotential within the current range investigated and the smallest interfacial resistance at OCV. At the same current density, the overpotential of SSC–SDC10(950) was about 1/3 of SSC–SDC10(1000) and 1/2 of SSC–SDC10(900). Fig. 4b also shows SSC–SDC10(950) to have the best performance, especially at current density over 150 mA/cm^2. However, at low current range, the overpotential of SSC–SDC10(950) was higher than that of SSC–SDC10(900). The firing temperature affects the microstructure, the adhesion of the electrode to the electrolyte, and the reactivity between SSC and SDC, and therefore, affects the active sites with respect to the oxygen reduction process in the cathode. Fig. 6a, b, and c shows typical cross-sectional SEM images of SSC–SDC10 cathodes fired at 900, 950, and 1000 °C, respectively. The grain size increases as expected with firing temperature. It was noted that SSC–SDC10(1000) had grains with much larger size (about four times) than SSC–SDC10 (950).The dramatic increase in grain size caused much low porosity and low specific area in the

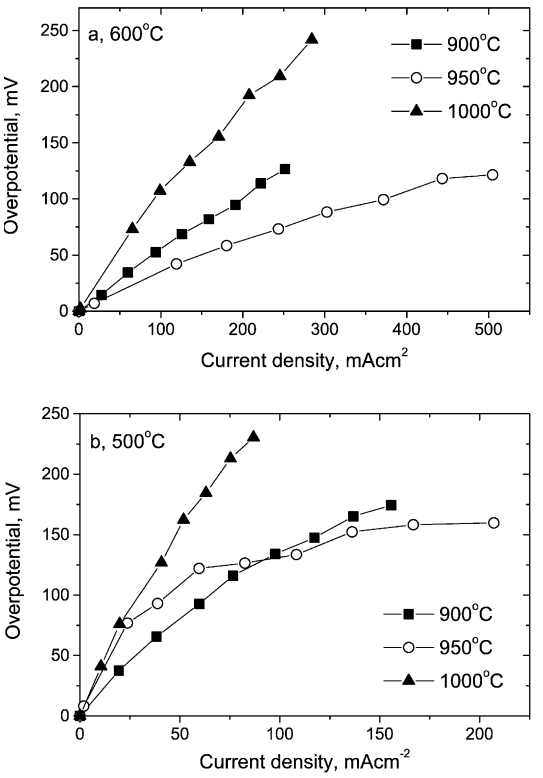

Fig. 4. Overpotential curves obtained at (a) 600 °C and (b) 500 °C for SSC–SDC10 cathodes fired at 900, 950, and 1000 °C for 4 h.

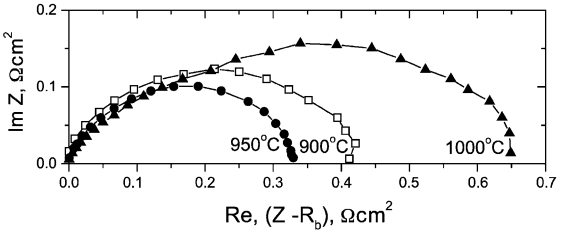

Fig. 5. Impedance spectra under open circuit conditions at 600 °C for SSC–SDC10 cathodes that fired at 900–1000 °C for 4 h.

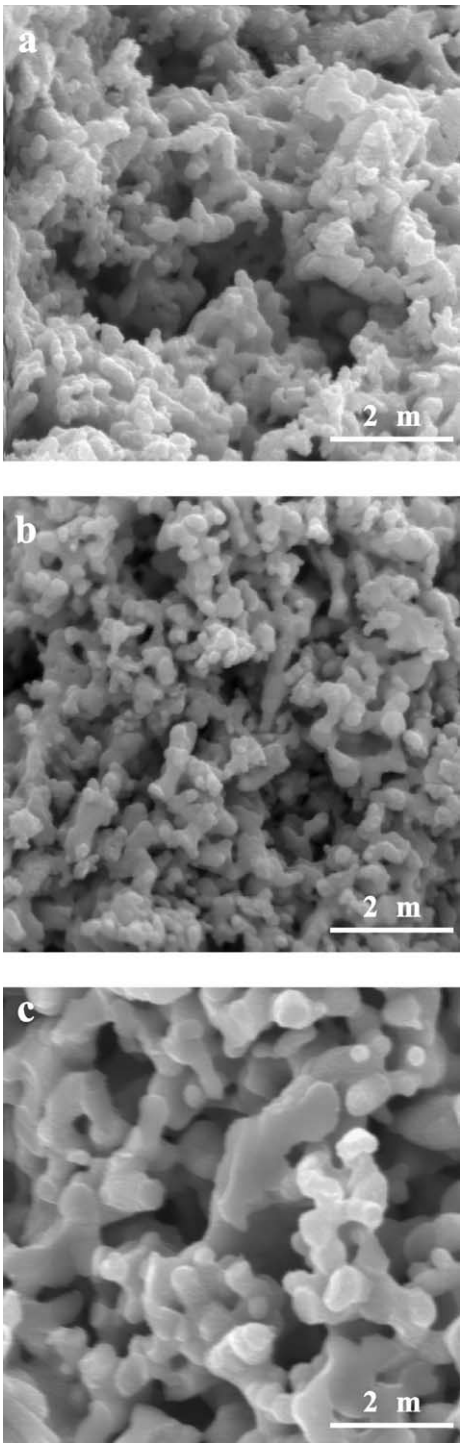

Fig. 6. Cross-sectional views (SEM images) of SSC–SDC10 cathodes fired at (a) 900 °C, (b) 950 °C, and (c) 1000 °C.

SSC–SDC10(1000) samples. The specific area was 2.20 m^2/g for SSC–SDC10(950) and decreased to 1.58 m^2/g for SSC–SDC10(1000). The average thickness of SSC–SDC10(950) cathode was about 40 μm. It decreased to 30 μm when the sample was further fired at 1000 °C for 4 h. This infers that further firing causes a dramatic loss of porosity, which might limit gas transportation to and from the reaction sites. It is recognized that the dense SSC cathodic performance is limited by the adsorption–desorption rates at the surface of the electrode [19]. However, it is believed that the heterogeneous chemical reactions within the electrode limit the performance of a porous mixed conducting oxide electrode [8]. The reaction rate is known to be a function of microstructural variables such as the particle size and surface area of the electrocatalyst. The relatively low specific area, large particle size and low porosity of SSC–SDC10(1000) should be the main factors to which the relatively high overpotential would be attributed. On the contrary, the grains of the cathode fired at 900 °C had only a slightly smaller size than that at 950 °C as observed from the cross-sectional views of SEM images. The specific area of SSC–SDC10(900) was 3.49 m^2/g, higher than that of SSC–SDC10(950). Finally, the porosity of cathode fired at 900 °C should be higher than that fired at 950 °C. However, SSC–SDC10 (900) cathode had higher interfacial resistances and higher overpotential than SSC–SDC10(950). It might be the relatively low firing temperature which caused poor adherence between the SDC electrolyte and the composite cathode, and consequently, bad bonding at the interface, leading to a higher charge transfer resistance. Actually, it was noted that the SSC–SDC10(900) cathode was very easy to peel off the electrolyte, and partial detachment of the cathode layer was observed under SEM after the cell testing.

Shown in Fig. 7 is the dependence of cell voltages and power densities on current densities of cells tested at 500 °C with SSC–SDC10 cathodes fired at different temperatures. A maximum power density of 120 mW/cm^2 was produced from the cell with the SSC–SDC10(950) cathode and was much higher than those with SSC–SDC10(900) cathode (60 mW/cm^2) and SSC–SDC10(1000) cathode (50 mW/cm^2). The area-specific resistance (Ω cm^2) as a function of temperature for SSC–SDC10 composite cathodes fired at

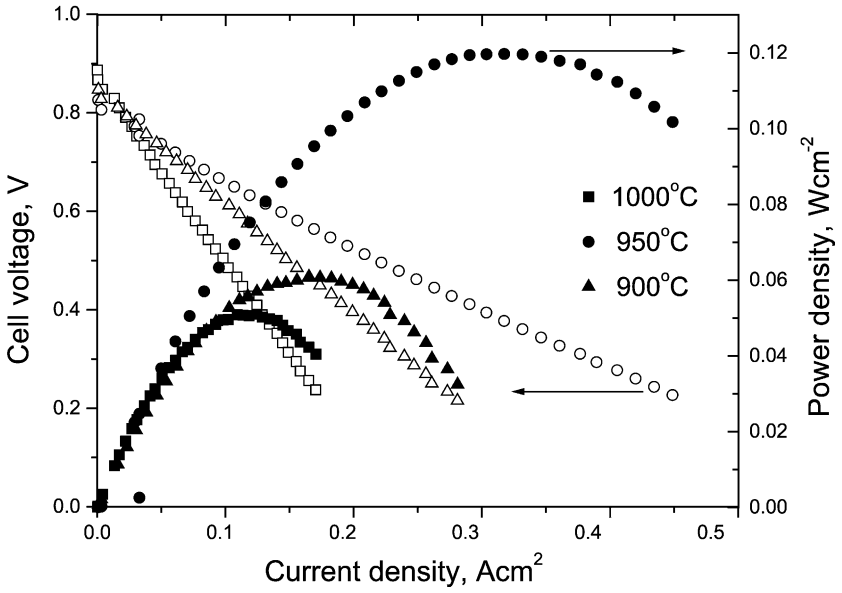

Fig. 7. The $I-V$ curves (open symbols) and the corresponding power densities (solid symbols) at 500 °C for a cell using SSC–SDC10 cathodes that fired at 900, 950, and 1000 °C when humidified hydrogen was used as fuel and stationary air as oxidant.

900–1000 °C is shown in Fig. 8. A single slope implies that the same reaction mechanism controls the overall electrode behavior at 400–600 °C. As can be observed in Fig. 8, the two-phase cathode fired at 900–1000 °C presented a clear minimum at 950 °C. This corresponds very well with the results of over-potential (Fig. 4) and fuel cell performance (Fig. 7) measurements. Fig. 8 also shows that at this optimized temperature, an even further reduction of resistance down to less than 0.18 Ω cm^2 at 600 °C is obtained with the addition of 30 wt.% SDC phase, which corresponds to the percolation limit.

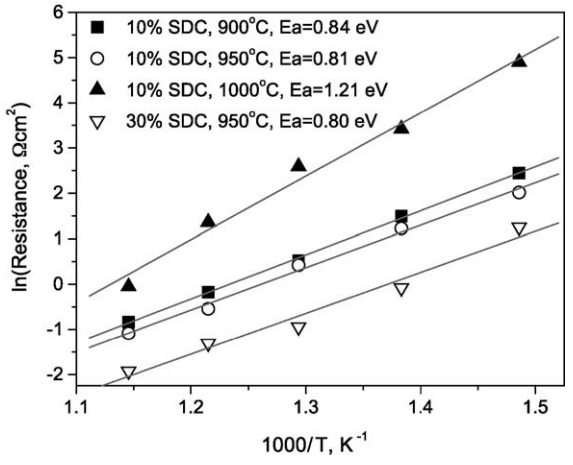

Fig. 8. Arrhenius plots of area-specific resistance of SSC composite electrodes sintered at temperatures from 900 to 1000 °C.

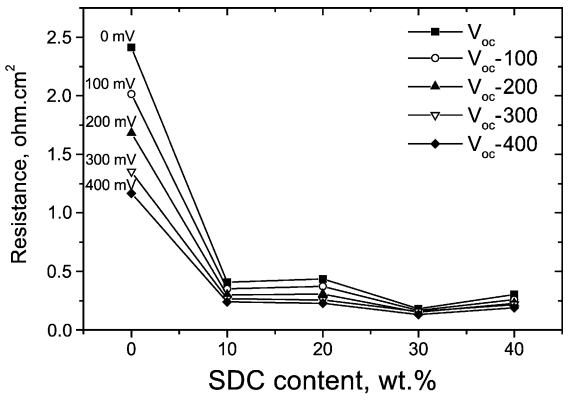

Fig. 9. The dependence of interfacial resistance on the SDC content of the SSC–SDC cathodes fired at 950 °C for 4 h. The data was measured at 600 °C when voltages of 0, −100, −200, −300, and −400 mV were applied to the cathodes.

3.4. Effect of SDC content

Fig. 9 summarizes the interfacial resistance, Rc (i.e. the difference between the real axis intercepts of the impedance arcs), for the SSC–SDC cathodes that consisted of different amounts of SDC. The impedances were measured at 600 °C by applying 0, −100, −200, −300, and −400 mV (versus OCV) to the cathodes, which were fired at 950 °C for 4 h. In general, the overall size of the impedance arcs decreased as SDC concentration increased to up 30 wt.%. Further increasing SDC content above 30 wt.% caused increase in the interfacial resistance. The interfacial resistance was about 2.5 Ω cm^2 at 600 °C for pure SSC. Meanwhile, the optimal composition, SSC–SDC30, yielded Rc less than 0.18 Ω cm^2 at 600 °C. It is possible that the polarization resistance of the optimized composite electrode was decreased by extending the triple phase boundary, which resulted in much lower overpotentials toward oxygen reduction and by increasing the oxygen diffusion upon the addition of an ionic conducting phase (SDC). Fig. 10 shows the overpotential at 500 and 600 °C of these cathodes. The cathode consisting of SSC+30 wt.% SDC showed the lowest overpotential, or the best electrochemical performance at both 500 and 600 °C. The results are consistent with those reported by Dusastre and Kilner [11] who had studied the electrochemical properties of the interfaces between porous composites of $La_{0.6}Sr_{0.4}Co_{0.2}Fe_{0.8}O_3/Ce_{0.9}Gd_{0.1}O_2$ cathodes and $Ce_{0.9}Gd_{0.1}O_2$ electrolytes at 500–700 °C. The optimum $Ce_{0.9}$ $Gd_{0.1}O_2$ addition to $La_{0.6}Sr_{0.4}Co_{0.2}$-$Fe_{0.8}O_3$ was 30 wt.% (36% by volume), which resulted in an area-specific resistivity four times lower. The observed high performances of the composite electrodes at 30 wt.% electrolytes can be interpreted with the effective medium percolation theory, which predicts the ambipolar transport behavior of composite-mixed ionic–electronic conductors as a function of the volume fraction of each of the randomly distributed constituent phases [11].

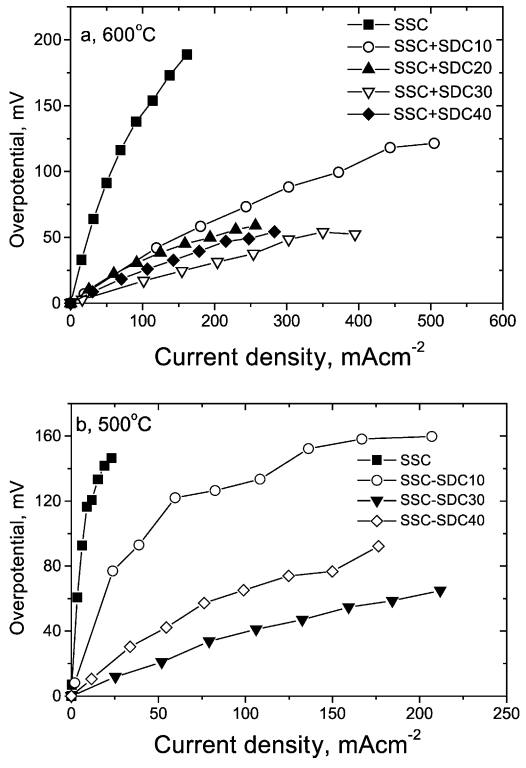

Fig. 10. Overpotential curves obtained at (a) 600 °C and (b) 500 °C for SSC cathodes containing 0, 10, 20, 30, and 40 wt.% SDC and fired at 950 °C for 4 h.

4. Conclusions

The cathodic resistances and overpotential of composite SSC–SDC cathodic materials were measured and found to exhibit good performance at low operating temperature depending on the weight fraction of SDC and the firing temperatures. Cathodes containing 10 wt.% SDC fired at 950 °C had an overpotential about two times lower than that fired at 900 °C and three times lower at 1000 °C. The development of a series of electrode microstructures produced by mixing an ionic conducting phase (SDC) with a mixed conducting phase (SSC) resulted in a significant reduction of the interfacial resistance from 2.0 Ω cm^2 for pure SSC to less than 0.18 Ω cm^2 at 600 °C under open circuit conditions, depending upon the distribution of the two phases. The composite containing 30% in weight SDC exhibited the lowest interfacial resistance or the highest catalytic activity for oxygen reduction, making this composite a promising cathode material for low-temperature solid oxide fuel cells based on SDC electrolytes.

Acknowledgements

The authors wish to gratefully acknowledge the support of this research by the National Science Foundation (Grant CTS-9819850), DOE-NETL (Grant DE-FG26-01NT41274), and the DARPA/DSO Palm Power program directed by Robert Nowak and funded through ARMY/ARO Grant DAAD19-01-1-0649 monitored by Richard Paur.

References

[1] J. Will, A. Mitterdorfer, C. Kleinlogel, D. Perednis, L.J. Gauckler, Solid State Ionics 131 (2000) 79–96.
[2] M. Mogensen, N.M. Sammes, G.A. Tompsett, Solid State Ionics 129 (2000) 63–94.
[3] C.R. Xia, M.L. Liu, J. Am. Ceram. Soc. 84 (8) (2001) 1903–1905.
[4] C.R. Xia, F.L. Chen, M.L. Liu, Electrochem. Solid-State Lett. 4 (5) (2001) A52–A54.
[5] C.R. Xia, M.L. Liu, Solid State Ionics 144 (2001) 249–255.
[6] S.C. Singhal, Solid State Ionics 135 (2000) 305–313.
[7] E.P. Murray, S.A. Barnett, Solid State Ionics 143 (2001) 265–273.
[8] B.C.H. Steele, Solid State Ionics 129 (2000) 95–110.
[9] R. Doshi, V.L. Richards, J.D. Carter, X. Wang, M. Krumpelt, J. Electrochem. Soc. 146 (1999) 1273–1278.
[10] E. Maguire, B. Gharbage, F.M.B. Marques, J.A. Labrincha, Solid State Ionics 127 (2000) 329–335.
[11] V. Dusastre, J.A. Kilner, Solid State Ionics 126 (1999) 163–174.
[12] I.C. Fullarton, J.A. Kilner, B.C.H. Steele, P.H. Middleton, Ionic and mixed conducting ceramics, in: T.A. Ramanarayanan, W.L. Worrell, H.L. Tuller (Eds.), 2nd International Symposium, The Electrochemical Society, vol. 94-12, 1994, pp. 9–26.
[13] H.Y. Tu, Y. Takeda, N. Imanishi, O. Yamamoto, Solid State Ionics 100 (1997) 283–288.
[14] T. Ishihara, M. Honda, T. Shibayama, H. Minami, H. Nishiguchi, Y. Takita, J. Electrochem. Soc. 145 (1998) 3177–3183.
[15] L.A. Chick, L.R. Pedersen, G.D. Maupin, J.L. Bates, L.E. Thomas, G.J. Exarhos, Mater. Lett. 10 (1990) 6.
[16] J. Winkler, P.V. Hendriksen, N. Bonanos, M. Mogensen, J. Electrochem. Soc. 145 (1998) 1184.
[17] M.L. Liu, Ionic and mixed conducting ceramics, in: T.A. Ramanarayanan, H.L. Tuller (Eds.), 1st International Symposium, The Electrochemical Society, vol. 91-12, 1991, pp. 191–209.
[18] M.L. Liu, H.X. Hu, J. Electrochem. Soc. 143 (6) (1996) L109.
[19] H. Fukunaga, M. Koyama, N. Takahashi, C. Wen, K. Yamada, Solid State Ionics 132 (2000) 279–285.